The effects of atmospheric turbulence and misalignment fading on performance of serial relaying M-ary PPM FSO systems with partially coherent Gaussian beam

Journal:	*IET Communications*
Manuscript ID:	COM-2013-0721.R1
Manuscript Type:	Research Paper
Date Submitted by the Author:	28-Jan-2014
Complete List of Authors:	Pham, Hien; Posts & Telecommunications Institute of Technology, Department of Wireless Communications Dang, Ngoc; Posts & Telecommunications Institute of Technology, Department of Optical Communications Pham, Anh; The University of Aizu, Computer Engineering
Keyword:	FREE-SPACE OPTICAL COMMUNICATION, OPTICAL WIRELESS, OPTICAL COMMUNICATION
Note: The following files were submitted by the author for peer review, but cannot be converted to PDF. You must view these files (e.g. movies) online.	
paper.tex	

The effects of atmospheric turbulence and misalignment fading on performance of serial relaying M-ary PPM FSO systems with partially coherent Gaussian beam

Hien T. T. Pham, Ngoc T. Dang and Anh T. Pham

Abstract

In this paper, we present a novel method to analyze the effects of atmospheric turbulence and misalignment fading (or pointing error) on performance of serial relaying M-ary pulse-position modulation (PPM) free-space optical (FSO) systems. Our study is more comprehensive than previous ones since we take into account the effect of beam size variation due to turbulence by using the partially coherent Gaussian beam model. In addition, we formulate a closed-form expression for bit-error rate (BER) of serial relaying M-ary PPM FSO systems over Gamma-Gamma atmospheric turbulence channel taking into account the effects of atmospheric attenuation, extinction ratio, and signal-dependent noise. We find that the laser source's coherent parameter, which governs the beam size at the receiver, plays an important role in the system design. If this parameter is not chosen properly, the system impairment will be either dominated by pointing error or geometric spreading loss. Thanks to the use of serial relaying and M-ary PPM, the effects of atmospheric turbulence and misalignment fading is mitigated hence the ability of combating atmospheric turbulence and the transmission distance of FSO systems are significantly improved. In addition, useful information for system design, such as the required number of relays for a specific turbulence strength and transmission distance, could be obtained from the numerical results.

Index Terms

Free-space optical communication, serial relaying, atmospheric turbulence, partial coherent source, gamma-gamma distribution.

I. Introduction

Free-space optical communication (FSO) is a line-of-sight (LOS) technology that enables data transmission based on the propagation of light in free space. Compared to radio frequency (RF) channel, FSO one provides high data rates, unregulated bandwidth, high security, and low power [1]. Since FSO is capable of providing Gigabit-per-second (Gbps) data rates, it has recently received much attention in first-mile access environments [2].

Manuscript received ; revised .

Although FSO systems have many advantages, a number of impairments, however, should be considered in the design of FSO systems. One such impairment comes from the effect of atmospheric turbulence, which is caused by the variations in the refractive index due to inhomogeneties in temperature and pressure changes [3]. Atmospheric turbulence is often modeled by using log-normal or Gamma-Gamma distribution, where Gamma-Gamma distribution has been found to be a good choice as it can accurately described weak to strong turbulence conditions [4]-[6]. Another impairment of FSO systems is pointing error caused by the misalignment between the transmitter and receiver [7]. All above impairments may result in rapid fluctuations in the intensity and phase of received signal [8]. Finally, atmospheric attenuation induced by absorption and scattering of photons by different aerosols and gaseous molecule in the atmosphere should also be considered [9].

To deal with problems induced by above-mentioned impairments, relay transmission has been proposed to FSO systems. Two typical relay configurations, including (1) serial relay transmission (i.e., multihop transmission) and (2) parallel relay transmission (i.e., cooperative diversity), can be employed in FSO systems. It is seen that relay-assisted FSO systems can provide more reliable transmission over longer distances. In addition, owing to relay transmission, it is possible to deploy FSO links between locations that do not have a line-of-sight.

A number of studies has been devoted to analyzing the performance of relay-assisted FSO systems [10]-[17]. Bit-error probability of multihop FSO systems has been investigated versus signal-to-noise ratio (SNR) by Akella et al. [10]. In this study, authors focus on the effect of different weather conditions on path loss without considering atmospheric turbulence. In [11], multihop transmission in weak turbulence conditions based on the log-normal channel model is studied by M. Safari et al. Also, the performance analysis of multihop FSO systems in strong turbulence conditions using Gamma-Gamma channel model can be found in [12]-[17].

In addition, misalignment between the transmitter and receiver due to building sway, which is also known as pointing error, is another performance degradation factor in FSO systems [18]. The effect of pointing error on the performance of relay-assisted FSO systems has been recently considered [14]-[17]. In these studies, the authors analyzed the outage probability, capacity, and bit-error rate (BER) for FSO systems using parallel, cooperative, and serial relaying under strong turbulence and pointing error conditions, respectively. The analyses were done for the systems using bit detect-and-forward (BDF) relaying and on-off keying (OOK) modulation considering the effect of additive white Gaussian noise (AWGN), which is assumed to be signal-independent. In addition, in all previous studies, authors also assumed that the laser beam size at the receiver was fixed (to 2.5 m at the distance of 1 km) [14], [17], [18].

The beam size is however not constant, especially under the impact of atmospheric turbulence. According to the partially (spatially) coherent Gaussian beam model, the beam size at the receiver is a function of several parameters, including the transmission distance, the index of refraction structure parameter C_n^2, and the source coherent parameter ζ_S [19]. Remarkably, ζ_S is an important factor for system design as it can be adjusted by using a phase diffuser located at the transmitter in order to obtain a desired beam size at the receiver. As partially coherent beam is practically suitable for FSO systems due to its increased beam size, the impact of atmospheric turbulence, source coherent parameter as well as link distance on the performance of FSO systems should be clarified for the

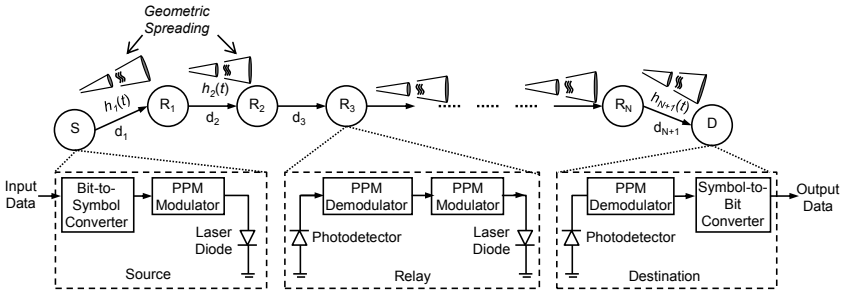

Fig. 1. Serial relaying FSO systems using M-ary PPM.

performance optimization.

In this paper, we therefore propose a novel method to analyze the effects of atmospheric turbulence and misalignment fading on the performance of serial relaying FSO systems. Our study is more comprehensive than previous ones since we take into account the effect of beam size variation due to turbulence. In particular, we employ the partially coherent Gaussian beam model for the laser source so that the beam size variation at the receiver could be considered. We formulate the closed-form expression for BER of the serial relaying FSO system over Gamma-gamma atmospheric turbulence channel. The degree of misalignment fading corresponding to different values of ζ_S, the transmission distance, and C_n^2, therefore, will be included in our analysis. Unlike previous studies which often use two-level modulation, e.g., OOK or binary pulse-position modulation (BPPM), we employ M-ary PPM to achieve better performance. All relays are based on symbol detect-and-forward technique, which is simpler than bit detect-and-forward and decode-and-forward ones. Furthermore, we consider signal-dependent shot noise, which results in more accurate analysis than that of previous studies [10]-[17]. Finally, also for the more accurate analysis, the effect of extinction ratio [20], which is caused by non-zero off-state of the laser, is taken into account.

The rest of the paper is organized as follows. The model of serial relaying M-ary PPM FSO systems is introduced in Section II. Section III presents the mathematical model of FSO channel. In Section IV, we formulate the BER of serial relaying M-ary PPM FSO systems. Section V shows the numerical results and discussion. Finally, Section VI concludes the paper.

II. System Model

A model of serial relaying M-ary PPM FSO system is shown in Fig. 1. The source (S) transmits the data signal to the destination (D) indirectly with the help of N serial intermediate terminals called relays (R). At the source, input data is first divided into blocks of b bits. Each block is then mapped to one of M possible symbols $(s_0, s_1, ..., s_M)$, where $M = 2^b$. At the PPM modulator, symbol intervals, T_w, are divided into M time slots and an optical pulse with constant average power of P_t is sent in one of these M time slots while remaining $M-1$ time slots (i.e., non-signal time slot) are empty. However, due to non-zero power in off-state of the laser, there a signal with a

power of $P_n = r_{ex}P_t$ is transmitted in non-signal time slots, where r_{ex} is the extinction ratio [20]. It is worth noting that each time slot has the duration of $T_s = b/MR_b$, where R_b is the bit rate.

Assume that h_i is the channel state modeling the random attenuation of the propagation channel between the $(i-1)$-th node and the i-th node. The received signal (i.e., photo current at the output of the photodetector) at the i-th node can be modeled as

$$\mathrm{I}_i = \begin{bmatrix} I_i^s \\ I_i^n \end{bmatrix} = \begin{bmatrix} \Re P_t h_i + n_i^s \\ \Re P_t r_{ex} h_i + n_i^n \end{bmatrix} \tag{1}$$

where I_i^s and I_i^n are the received signal corresponding to signal and non-signal time slots of the PPM symbol. $\Re$ is the responsivity of photodiode. n_i^s and n_i^n denote the additive noise terms for the signal and non-signal time slots, respectively. Consider the effect of path loss (h_i^l), atmospheric turbulence (h_i^a), and pointing errors (h_i^p), the channel coefficient (h_i) can be described as

$$h_i = h_i^l h_i^a h_i^p. \tag{2}$$

At each relay or destination, the PPM symbols are detected by a PPM demodulator, where integrated photocurrents over M time slots are compared, and the position of the slot with the highest current determines the transmitted symbol. At the relays, detected symbol is re-modulated before retransmitting with an average power of P_t to the next relay or to the destination. Finally, at the destination, detected symbol is converted to the binary data by a symbol-to-bit converter.

III. Atmospheric Channel Model

A. Atmospheric Attenuation

The atmospheric channel attenuates the signal traversing it as a result of absorption and scattering processes. The concentrations of matter in the atmosphere, which result in the signal attenuation vary spatially and temporally, and will depend on the weather conditions. The attenuation of optical power through the atmospheric is described by the exponential Beers-Lambert Law as [9]

$$h_i^l = \exp\left(-a_l d_i\right), \tag{3}$$

where a_l is the attenuation coefficient and d_i is the transmission distance of the i-th hop (between the $i-1$-th node and the i-th node). This coefficient is considered as a fixed scaling factor during a long period of time.

B. Atmospheric Turbulence and Misalignment Fading Models

According to the commonly used turbulence model, the variations of the medium can be realized as individual cells of air or eddies of different diameters and refractive indices. In the context of geometrical optics, these eddies may be observed as lenses that randomly refract the optical wave-front, generating a distorted intensity profile at the receiver of a communication system. The intensity fluctuation is known as scintillation and represents one of the most important factors that limit the performance of an atmospheric FSO communication link.

In this paper, as we try to investigate the system performance in moderate-to-strong turbulence regime, Gamma-Gamma distribution will be used to model the atmospheric turbulence channel. The PDF of the intensity fluctuation (h_i^a) due to atmospheric turbulence is thus given by [21]

$$f_{h_i^a}(h_i^a) = \frac{2\left(\alpha_i\beta_i\right)^{(\alpha_i+\beta_i)/2}}{\Gamma\left(\alpha_i\right)\Gamma\left(\beta_i\right)}\left(h_i^a\right)^{\frac{\alpha_i+\beta_i}{2}-1} K_{\alpha_i-\beta_i}\left(2\sqrt{\alpha_i\beta_i h_i^a}\right),\ h_i^a > 0, \tag{4}$$

where $\Gamma(.)$ denotes Gamma function and $K_{\alpha_i-\beta_i}(.)$ is the modified Bessel function of the second kind of order $\alpha_i - \beta_i$. α_i and β_i are the effective number of small-scale and large-scale eddies of scattering environment, respectively. They are written as [21]

$$\begin{aligned}\alpha_i &= \left[\exp\left(\frac{0.49\sigma_R^2}{\left(1+1.11\sigma_R^{12/5}\right)^{7/6}}\right)-1\right]^{-1}\\ \beta_i &= \left[\exp\left(\frac{0.51\sigma_R^2}{\left(1+0.69\sigma_R^{12/5}\right)^{5/6}}\right)-1\right]^{-1}\end{aligned} \tag{5}$$

where $\sigma_{R,i}$ is the Rytov variance which is defined as

$$\sigma_{R,i}^2 = 1.23\left(\frac{2\pi}{\lambda}\right)^{7/6} C_n^2 d_i^{11/6}, \tag{6}$$

where λ is the wavelength. The unitless Rytov variance represents the strength of the turbulence, which is governed by the index of refraction structure parameter C_n^2 and the distance d_i. In general, C_2^n varies from 10^{-13} $\mathrm{m}^{-2/3}$ for strong turbulence to 10^{-17} $\mathrm{m}^{-2/3}$ for weak turbulence with 10^{-15} $\mathrm{m}^{-2/3}$ often defined as a typical average value [22].

In order to model misalignment fading, we consider a circular detection aperture of radius a and a Gaussian beam profile at the receiver. The probability distribution function (PDF) of h_i^p can be derived as [18]

$$f_{h_i^p}\left(h_i^p\right) = \frac{\gamma_i^2}{A_{0,i}^{\gamma_i^2}}\left(h_i^p\right)^{\gamma_i^2-1}, \tag{7}$$

where $\gamma_i = \omega_{z_{eq}}/2\sigma_{s,i}$ is the ratio between the equivalent beam radius ($\omega_{z_{eq}}$) and the pointing error displacement standard deviation ($\sigma_{s,i}$) at the receiver. $A_{0,i}$ is the fraction of the collected power at the center of the beam. According to [19], $\omega_{z_{eq}}$ and $A_{0,i}$ are given by

$$A_{0,i} = \left[\mathrm{erf}\left(v\right)\right]^2 \text{ and } \omega_{z_{eq}}^2 = \omega_{z,i}^2\frac{\sqrt{\pi}\mathrm{erf}\left(v\right)}{2v\exp\left(-v^2\right)}, \tag{8}$$

where $\mathrm{erf}\left(.\right)$ is the error function; $v = \left(\sqrt{\pi}a\right)/\left(\sqrt{2}\omega_{z,i}\right)$; and $\omega_{z,i}$ is beam radius of a Gaussian beam calculated at e^{-2} at distance d_i. For Gaussian beam propagating in atmospheric turbulence, $\omega_{z,i}$ can be approximated as [19]

$$\omega_{z,i} = \omega_0\left[1+\zeta\left(\frac{\lambda d_i}{\pi\omega_0^2}\right)^2\right]^{\frac{1}{2}}, \tag{9}$$

where ω_0 is the beam waist at $d_i = 0$, $\zeta = \left(\zeta_S + 2\omega_0^2/\rho_0^2(d_i)\right)$, and $\rho_0(d_i) = (0.55C_n^2k^2d_i)^{-3/5}$ is the coherence length. ζ_S is the source coherent parameter, which is equal to one for coherent beam. The value of ζ_S can be changed by placing a phase diffuser directly in front of the laser source.

C. Channel Statistical Model

The channel state h_i consists of three terms, where h_i^l is deterministic while h_i^a and h_i^p are random variables. With this assumption, the PDF of the channel state $h_i = h_i^l h_i^a h_i^p$ can be mathematically expressed as [18]

$$f_{h_i}(h_i) = \int f_{h_i|h_i^a}(h_i|h_i^a) f_{h_i^a}(h_i^a)\, dh_i, \tag{10}$$

where $f_{h_i|h_i^a}(h_i|h_i^a)$, which is presented more detail in [18], is the condition probability given h_i^a. As $f_{h_i^a}$ is Gamma-Gamma distribution, $f_{h_i}(h_i)$ is given by [18]

$$f_{h_i}(h_i) = \frac{2\gamma_i^2 (\alpha_i\beta_i)^{(\alpha_i+\beta_i)/2}}{\left(A_{0,i}h_i^l\right)^{\gamma_i^2}\Gamma(\alpha_i)\Gamma(\beta_i)} h_i^{\gamma^2-1}\int_{h_i/A_{0,i}h_i^l}^{\infty} (h_i^a)^{(\alpha_i+\beta_i)/2-1-\gamma_i^2} K_{\alpha_i-\beta_i}\left(2\sqrt{\alpha_i\beta_i h_i^a}\right) dh_i^a. \tag{11}$$

By expressing $K_{\alpha_i-\beta_i}(.)$ in terms of the Meijer's G-function, i.e., $K_\nu(x) = \frac{1}{2}G_{0,2}^{2,0}\left[x^2/4\middle|\begin{matrix}-\\ \frac{\nu}{2}, -\frac{\nu}{2}\end{matrix}\right]$ [23, Eq. (9.34.3)], and using [24, Eq. (07.34.21.0085.01)] for obtaining the closed-form expression for integral term, Eq. (11) is derived as

$$f_{h_i}(h_i) = \frac{\alpha_i\beta_i\gamma_i^2}{A_{0,i}h_i^l\Gamma(\alpha_i)\Gamma(\beta_i)}\left(\frac{\alpha_i\beta_i h_i}{A_{0,i}h_i^l}\right)^{\frac{\alpha_i+\beta_i}{2}-1} G_{1,3}^{3,0}\left[\frac{\alpha_i\beta_i h_i}{A_{0,i}h_i^l}\middle|\begin{matrix}1-\frac{\alpha_i+\beta_i}{2}+\gamma^2\\ -\frac{\alpha_i+\beta_i}{2}+\gamma^2, \frac{\alpha_i-\beta_i}{2}, \frac{-\alpha_i+\beta_i}{2}\end{matrix}\right]. \tag{12}$$

Finally, by using [24, Eq. (07.34.16.0001.01)] for making simplification, the final closed-form expression for $f_{h_i}(h_i)$ can be derived as

$$f_{h_i}(h_i) = \frac{\alpha_i\beta_i\gamma_i^2}{A_{0,i}h_i^l\Gamma(\alpha_i)\Gamma(\beta_i)} G_{1,3}^{3,0}\left[\frac{\alpha_i\beta_i}{A_{0,i}h_i^l}h_i\middle|\begin{matrix}\gamma_i^2\\ \gamma_i^2-1, \alpha_i-1, \beta_i-1\end{matrix}\right]. \tag{13}$$

IV. Performance Analysis

A. Signal to Noise Ratio

Electrical signal to noise ratio (SNR) at the i-th relay (or the destination) can be defined that

$$\text{SNR} = \frac{\left(\mu_i^s - \mu_i^n\right)^2}{\sigma_i^{s^2} + \sigma_i^{n^2}}, \tag{14}$$

where μ_i^s and μ_i^n are means of I_i^s and I_i^n, which can be derived from Eq. (1) as

$$\begin{bmatrix}\mu_i^s\\ \mu_i^n\end{bmatrix} = \begin{bmatrix}\Re P_t h_i\\ \Re P_t R_{ex} h_i\end{bmatrix}. \tag{15}$$

In Eq. (14), $\sigma_i^{s^2}$ and $\sigma_i^{n^2}$ are noise variance of receiver noises n_i^s and n_i^n, respectively. In this analysis, we just focus on the effect of signal-dependent shot noise, which are additive Gaussian noise with zero mean and variance as follows

$$\begin{bmatrix}\sigma_i^{s^2}\\ \sigma_i^{n^2}\end{bmatrix} = \begin{bmatrix}2e\Re P_t h_i \Delta f\\ 2e\Re P_t r_{ex} h_i \Delta f\end{bmatrix}, \tag{16}$$

where e is the electron charge and Δf is the effective noise bandwidth. For M-ary PPM, Δf is related to the bit rate R_b as $\Delta f = MR_b/(2\log_2 M)$ [20]. By substituting Eqs. (15) and (16) in Eq. (14), SNR can be computed as

$$\text{SNR} = \frac{\Re P_t (1-r_{rx})^2}{2e\Delta f (1+r_{rx})} h_i. \tag{17}$$

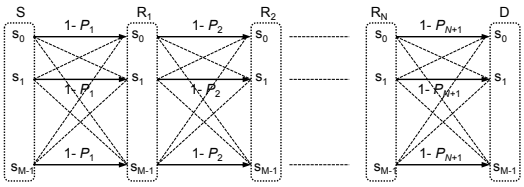

Fig. 2. Multihop equivalent channel model.

B. Bit Error Rate

In this subsection, symbol error probability of each hop is first calculated. Based on symbol error probability of each hop, we derived the total symbol error probability of multihop FSO link and then the BER of multihop FSO systems.

Denoting P_i as the symbol error probability of the i-th hop (i.e., at the i-th node with $i = 1, 2, ..., N + 1$). We assume that the transmitted data is large enough that the probabilities of sending any symbols are the same. Without the loss of generality, we also assume that symbol s_0 is transmitted. By using union bound technique, the upper bound to the instantaneous symbol error probability can be expressed as

$$\begin{aligned} P_i &\leq 1 - \Pr\{I_i^0 > I_i^u | u \in \{1, ..., M-1\}, s = s_0\} \\ &\leq \sum_{u=1}^{M-1} \Pr\{I_i^u \geq I_i^0 | s = s_0\} = (M-1)\Pr\{I_i^n \geq I_i^s\} \\ &\leq \frac{M-1}{2} \int_0^\infty f_{h_i}(h_i) \text{erfc}\left(\sqrt{\frac{\text{SNR}}{2}}\right) dh_i, \end{aligned} \tag{18}$$

where s represents the transmitted symbol. I_i^u is the current corresponding to time slot u and erfc(.) is the complementary error function.

By substituting Eq. (13) in Eq. (18) and expressing erfc(.) as Meijer's G-function [24, Eq.(06.27.26.0006.01)], we can obtain

$$\begin{aligned} P_i &\leq \frac{(M-1)\,\alpha_i \beta_i \gamma_i^2}{2\sqrt{\pi} A_{0,i} h_i^l \Gamma(\alpha_i)\,\Gamma(\beta_i)} \\ &\quad \times \int_0^\infty G_{1,3}^{3,0}\left[\frac{\alpha_i \beta_i}{A_{0,i} h_i^l} h_i \middle| \begin{matrix} \gamma_i^2 \\ \gamma_i^2 - 1, \alpha_i - 1, \beta_i - 1 \end{matrix}\right] G_{1,2}^{2,0}\left[\frac{\Re P_t (1 - r_{rx})^2}{4e\Delta f (1 + r_{rx})} h_i \middle| \begin{matrix} 1 \\ 0, \frac{1}{2} \end{matrix}\right] dh_i^a. \end{aligned} \tag{19}$$

Next, based on [24, Eq. (07.34.21.0011.01)], a closed-form expression for the symbol error probability is derived as

$$P_i \leq \frac{(M-1)\,\gamma_i^2}{2\sqrt{\pi}\Gamma(\alpha_i)\,\Gamma(\beta_i)} G_{4,3}^{2,3}\left[\frac{\Re P_t (1 - r_{rx})^2 A_{0,i} h_i^l}{4e\Delta f (1 + r_{rx})\,\alpha_i \beta_i} \middle| \begin{matrix} 1 - \gamma_i^2, 1 - \alpha_i, 1 - \beta_i, 1 \\ 0, \frac{1}{2}, \gamma_i^2 \end{matrix}\right]. \tag{20}$$

The multihop FSO system with $N+1$ hops (i.e., N relays) is modeled as a concatenation of $N+1$ M-symmetric channel with an error probability P_i for the i-th hop (see Fig. 2). Assuming that each hop is independent, the end-

TABLE I

SYSTEM PARAMETERS AND CONSTANTS.

Name	Symbol	Value
PD responsivity	$\Re$	0.8 A/W
Extinction ratio	r_{ex}	0.05
Outer scale of turbulence	L_0	10 m
Attenuation coefficient	a_l	0.1 km^{-1}
Beam waist at $d_i = 0$	ω_0	2.5 cm
Bit rate	R_b	5 Gbps
Wavelength	λ	1550 nm

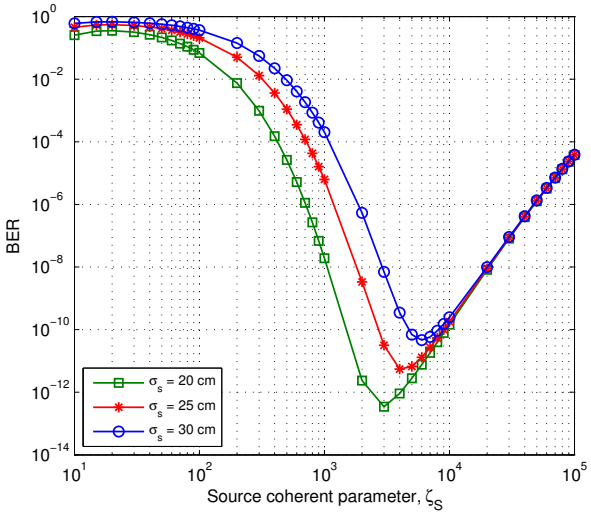

Fig. 3. BER versus the source coherent parameter with BPPM, $P_s = 0$ dBm, $L = 5$ km, $N = 3$, $2a = 20$ cm, and $C_n^2 = 10^{-14}$.

to-end symbol error probability (P_e) is given by

$$P_e = 1 - \prod_{i=1}^{N+1} (1 - P_i)\,. \tag{21}$$

Once the PPM symbol is detected, it is mapped to a string of $\log_2(M)$ bits via the inverse of the encoding mapping. There are $M/2$ symbol errors that will produce an error in a given bit in the string, and there are $M - 1$ unique symbol errors. Thus, assuming all symbol errors are equally likely, the resulting bit error rate (BER) can be expressed as

$$\text{BER} = \frac{M}{2\,(M-1)} P_e. \tag{22}$$

V. Numerical Results

In this section, we investigate the BER of serial relaying FSO systems using M-ary PPM with the total transmission distance of L km. We assume the consecutive nodes are equidistant along the path from the source to the destination. To have a fair comparison to conventional single-hop FSO system using OOK or BPPM, the analysis is considered under a constraint on the average power per bit denoted as P_s, which is related to the average transmitted-power per time slot (P_t) as

$$P_t = \frac{M \log_2 M}{(N+1)} P_s, \tag{23}$$

where $N+1$ is the number of hops. In addition, we assume jitter standard deviation a linear function of distance thus $\sigma_{s,i}$ can be obtained from the jitter standard deviation at 1 km (σ_s) and the distance of i-th hop (d_i) as $\sigma_{s,i} = \sigma_s d_i$.

The system parameters used in the analysis are shown in Table I, where the values of PD responsivity and extinction ratio are chosen based on the parameters a typical photodiode and laser source, respectively [20]. The attenuation coefficient is fixed to 0.1 km^{-1}, which is corresponding to a clear weather condition. The system's performance will be investigated in the moderate-to-strong turbulence regime, where C_n^2 ranges from 10^{-15} to 10^{-13}. We use the collimated beam with $\omega_0 = 2.5$ cm in combination with a phase diffuser to govern the value of ζ_S [19]. In addition, both bit rate and link distance used in our analysis are larger than those of a typical FSO systems in order to show the advantages of using serial relay and M-ary PPM.

In Fig. 3, BER is evaluated versus the source coherent parameter, ζ_S, which is in proportional to the beam size at the receiver, i.e. the higher ζ_S, the bigger beam size we have. The FSO system under consideration uses BPPM with the transmitted power per bit of 0 dBm. It is seen that BER response for a range of ζ_S values is divided into two regions, which are distinguished by an optimum value at which the lowest BER is achieved. In the first region where ζ_S is smaller than the optimum value, the effect of pointing errors is dominant. As a result, BER varies strongly when jitter standard deviation is changed. In this region, it is necessary to increase ζ_S (or the beam size) to reduce the effect of pointing errors. In the second region where ζ_S is larger than the optimum value, the effect of pointing errors is negligible since the beam size is relatively larger than the detector area and the jitter standard deviation. Consequentially, the variation of jitter standard deviation does not affect on BER. In this case, if ζ_S increases (i.e., the beam size increases), the fraction of the collected power will reduce and BER increases since geometric spreading loss increases.

Next, we investigate BER versus the source coherent parameter with different values of detection aperture diameter (i.e., $2a$). Figure 4 shows that the increase of aperture diameter helps to reduce BER significantly thanks to the reduction of pointing error loss and especially geometric spreading loss. Similar to the previous result, there is an optimum value of ζ_S corresponding to each value of aperture diameter. Also, the range of ζ_S values satisfying a required level of BER (e.g., BER = 10^{-9}) can be obtained from this figure. When aperture diameter is large, the range of ζ_S values is extended thus it is easier for system design.

The benefits of using M-ary PPM and serial relaying to mitigate the effect of turbulence are shown in Fig. 5. The performance of proposed FSO system is compared to that of a no-relaying OOK one with a typical distance

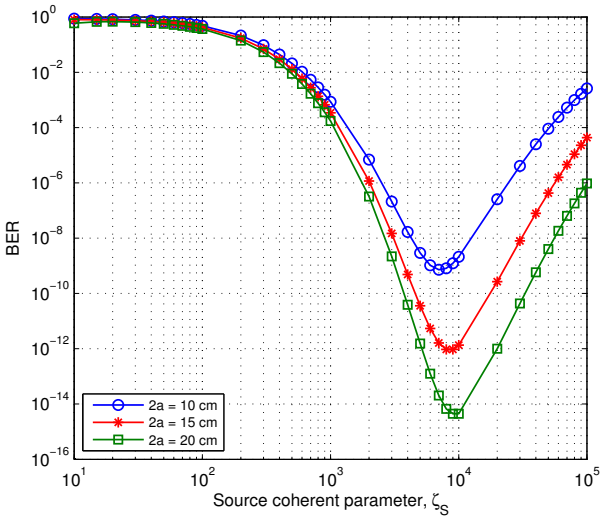

Fig. 4. BER versus the source coherent parameter with BPPM, $P_s = 0$ dBm, $L = 5$ km, $N = 3$, $\sigma_s = 30$ cm, and $C_n^2 = 5 \times 10^{-15}$.

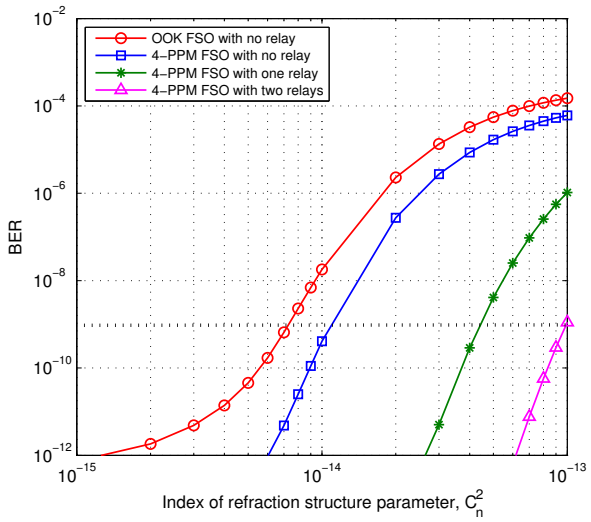

Fig. 5. BER versus the index of refration structure parameters, $P_s = 0$ dBm, $L = 2$ km, $2a = 20$ cm, $\sigma_s = 30$ cm, and $\zeta_S = 4000$.

of 2 km and the bit rate of 5 Gbps. It is seen that the performance improvement of using M-ary PPM (without relaying) is considerable only when turbulence is not so strong (e.g., in moderate turbulence regime). In strong turbulence regime, serial relaying should be used as it help to significantly improve the system performance. For example, in strong turbulence condition with $C_n^2 = 10^{-13}$, 4-PPM FSO system with 2 relays can provide the BER of 10^{-9}, which is much lower than BER $= 10^{-4}$ that is supported by no-relaying OOK FSO system.

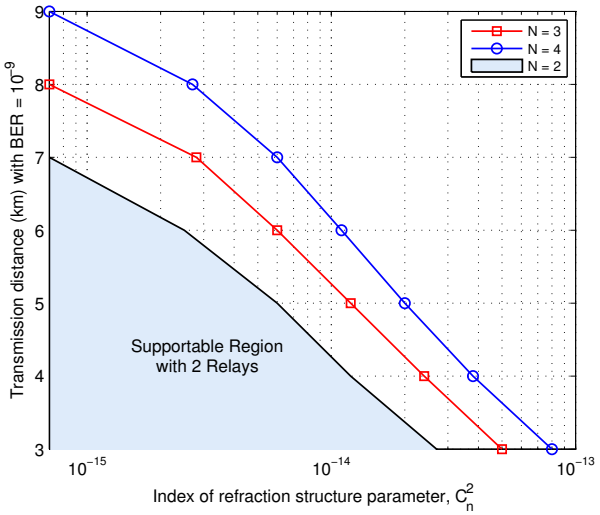

Fig. 6. Transmission length (at BER = 10^{-9}) versus index of refraction structure parameter with BPPM, $P_s = 0$ dBm, $2a = 20$ cm, $\sigma_s = 35$ cm, and $\zeta_S = 4000$.

Figure 6 shows that the maximum transmission length with BER = 10^{-9} of BPPM FSO systems is improved significantly thanks to serial relaying. When the number of hop (N) increases from 2 to 4, the maximum transmission distance increases from 7 km to 9 km at $C_n^2 = 7 \times 10^{-16}$, respectively. For a specific transmission length, the use of serial relaying helps to improve the ability of FSO systems in combating against atmospheric turbulence. With the transmission distance of 7 km, the turbulence strength that FSO systems can suffer increase from $C_n^2 = 7 \times 10^{-16}$ to $C_n^2 = 6 \times 10^{-15}$ when N increases from 2 to 4.

The required number of relays for a specific turbulence strength and transmission distance can also be determined by using Fig. 6. For example, with the transmission distance of 5 km and $C_n^2 = 10^{-14}$, at least three relays need to be used in order to have the BER of 10^{-9}. The supportable region in terms of transmission distance and turbulence strength corresponding to a specific number of relays hence can be demonstrated as shown in the figure.

VI. Conclusions

We have presented a novel method to formulate closed-form expression for BER of serial relaying FSO systems using M-ary PPM over Gamma-Gamma atmospheric turbulence and misalignment fading channels. Thanks to the use of the partial coherent Gaussian beam model, the effect of beam size variation due to turbulence can be considered. Other physical layer impairments were also taken into consideration including atmospheric attenuation and signal-dependent shot noise. The numerical results helped to determine the value of coherent parameter properly to reduce the effect of misalignment fading. The benefits of using serial relaying and M-ary PPM in combating atmospheric turbulence and extending the transmission distance were also quantified in this paper. Moreover,

useful information for system design, such as the required number of relays for a specific turbulence strength and transmission distance, could be obtained from the numerical results.

ACKNOWLEDGMENT

The authors would like to thank the reviewers for their through reviews and useful suggestions for improving the readability of this paper. This research was supported by the Vietnam's National Foundation for Science and Technology Development (NAFOSTED) under grant number 102.02-2013.02.

REFERENCES

[1] Heatley, D.J., Wisely, D.R. , Neild, I. , and Cochrane, P.: 'Optical wireless: The story so far', *IEEE Commun. Mag.*, 1998, **36**, (12), pp. 72–82

[2] Liu, Q., Qiao, C. , Mitchell, G., and Stanton, S.: 'Optical wireless communication networks for first- and last-mile broadband access [Invited]', *J. Opt. Netw.*, 2005, **4**, (12), pp. 807–828

[3] Zhu, X. and Khan, J.M.: 'Free-space optical communication through atmospheric turbulence channels', *IEEE Trans. Commun.*, 2002, **50**, (8), pp. 1293–1300

[4] Al-Habash, M.A., Andrews, L.C., and Phillips, R.L.: 'Mathematical model for the irradiance probability density function of a laser beam propagating through turbulent media', *Opt. Eng.*, 2001, **40**, (8), pp. 1554–1562

[5] Uysal, M., Jing, L., and Meng, Y.: 'Error rate performance analysis of coded free-space optical links over gamma-gamma atmospheric turbulence channels', *IEEE Trans. Wireless Commun.*, 2006, **5**, (6), pp. 1229–1233

[6] Nistazakis, H.E., Tombras, G.S.: 'On the use of wavelength and time diversity in optical wireless communication systems over gamma-gamma turbulence channels', *Optics & Laser Technology*, 2012, **44**, (7), pp. 2088-2094

[7] Kedar, D. and Arnon, S.: 'Urban optical wireless communications networks: The main challenges and possible solutions', *IEEE Commun. Mag.*, 2003, **42**, (5), pp. 2–7

[8] Davis, C.C. and Smolyaninov, I.: 'The effect of atmospheric turbulence on bit-error-rate in an on-off keyed optical wireless system', *Proc. SPIE Free-Space Laser Commun. Laser Imaging*, 1997, pp. 126–137

[9] Naboulsi, M.A., Sizum,H., and de Fornel, F.: 'Fog attenuation prediction for optical and infrared waves', *Opt. Eng.*, 2004, **43**, (2), pp. 319–329

[10] Akella, J., Yuksel, M., and Kalyanaraman, S.: 'Error analysis of multi-hop free-space optical communication', *Proc. of IEEE International Conference on Commun.*, 2005, pp. 1777–1781

[11] Safari, M. and Uysal, M.: 'Relay-assisted free-space optical communication', *IEEE Trans. Wireless Comm.*, 2008, **7**, (12), pp. 5441–5449

[12] Tsiftsis, T.A., Sandalidis, H.G., Karagiannidis, G.K., and Sagias ,N.C.: 'Multihop free-space optical communications over strong turbulence channels,' *Proc. of IEEE International Conference on Commun.*, 2006, pp. 2755–2759

[13] Datsikas, C.K., Peppas, K.P., Sagias, N.C., and Tombras, G.S.: 'Serial free-space optical relaying communications over Gamma-Gamma atmospheric turbulence channels', *J. Opt. Commun. Netw.*, 2010, **2**, (8), pp. 576–586

[14] Feng, M., Wang, J.B., Sheng, M., Cao, L.L., Xie X.X., and Chen, M.: 'Outage performance for parallel relay-assisted free-space optical communications in strong turbulence with pointing errors', *Proc. of International Conference on Wireless Commun. and Signal Processing (WCSP)*, 2011, pp. 1–5

[15] Peppas, K.P.'' 'Capacity Analysis of Dual Amplify-and-Forward Relayed Free-Space Optical Communication Systems over Turbulence Channels with Pointing Errors', *J. Opt. Commun. Netw.*, 2013, **5**, (9), pp. 1032–1042

[16] Antonio, G.Z., Carmen, C.V., Beatriz, C.V., Ruben B.R.: 'Bit detect and forward relaying for FSO links using equal gain combining over gamma-gamma atmospheric turbulence channels with pointing errors' *Optics Express*, 2012, **20**, (15), pp. 16394–16409

[17] Sheng, M., Jiang, P., Hu, Q., Su, , and Xie, X.: 'End-to-end average BER analysis for multihop free-space optical communications with pointing errors', *J. Opt.*, 2013, **15**, (055408), pp. 1–7

[18] Farid, A.A. and Hranilovic, S.: 'Outage capacity optimization for free-space optical links with pointing errors', *IEEE J. Lightw. Technol.*, 2007, **25**, (7), pp. 1702–1710

[19] Ricklin, J.C. and Davidson, F.M.: 'Atmospheric turbulence effects on a partially coherent Gaussian beam: Implications for free space laser communication', *J. Opt. Soc. Amer. A, Opt. Image Sci.*, 2002, **19**, (9), pp. 1794–1802

[20] Agrawal, Govind P.: 'Fiber-optic communication systems' (Ed Wiley, 2002)

[21] Djordjevic, I., Ryan, W., Vasic, B.: 'Coding for Optical Channels' (Springer, 2010)

[22] Andrews, LC., Philips, RL.: 'Laser beam propagation through random media' (SPIE Optical Engineering Press, Bellingham, WA, 1998)

[23] Gradshteyn, I. S. and Ryzhik, I.M.: 'Table of Integrals, Series, and Products' (New York: Academic, 2007, 7th ed.)

[24] Wolfram. (2001) The Wolfram functions site. Internet. [Online]. Available: http://functions.wolfram.com

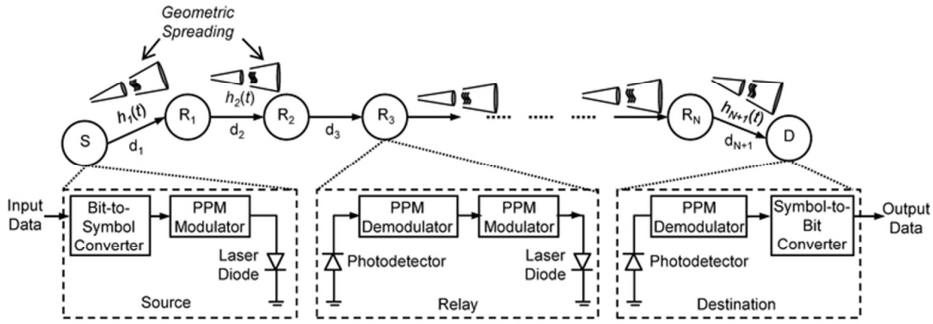

66x23mm (300 x 300 DPI)

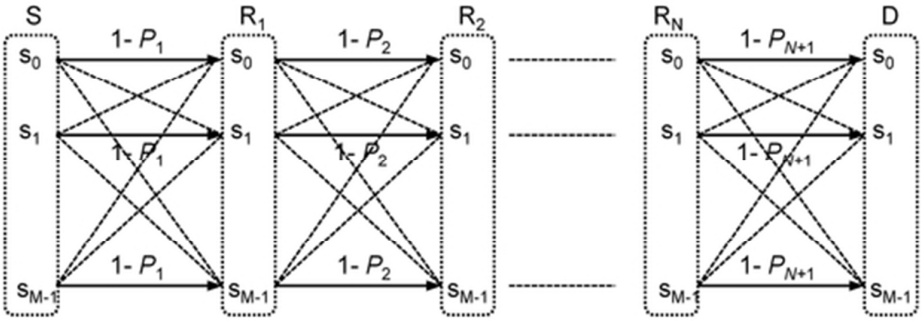

45x15mm (300 x 300 DPI)

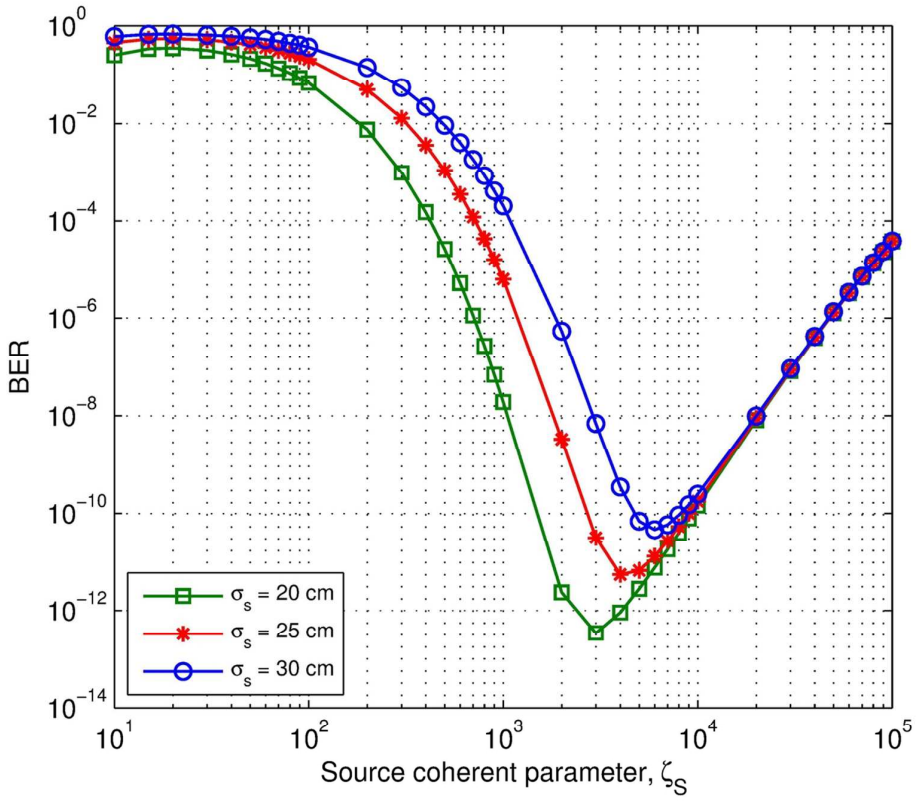

108x96mm (300 x 300 DPI)

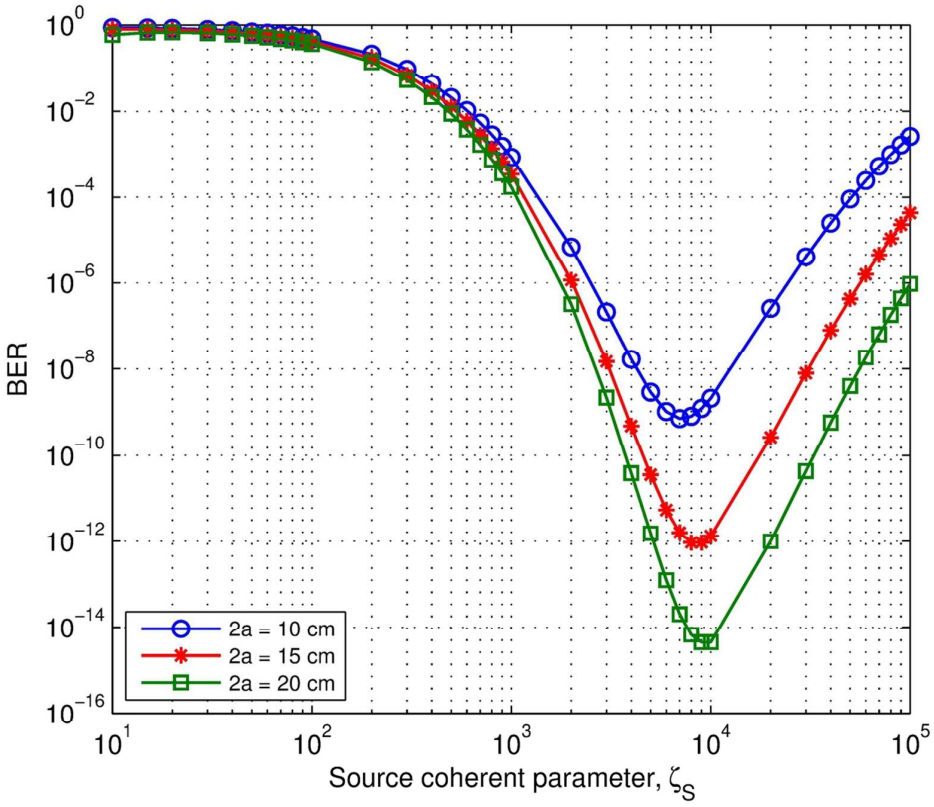

108x96mm (300 x 300 DPI)

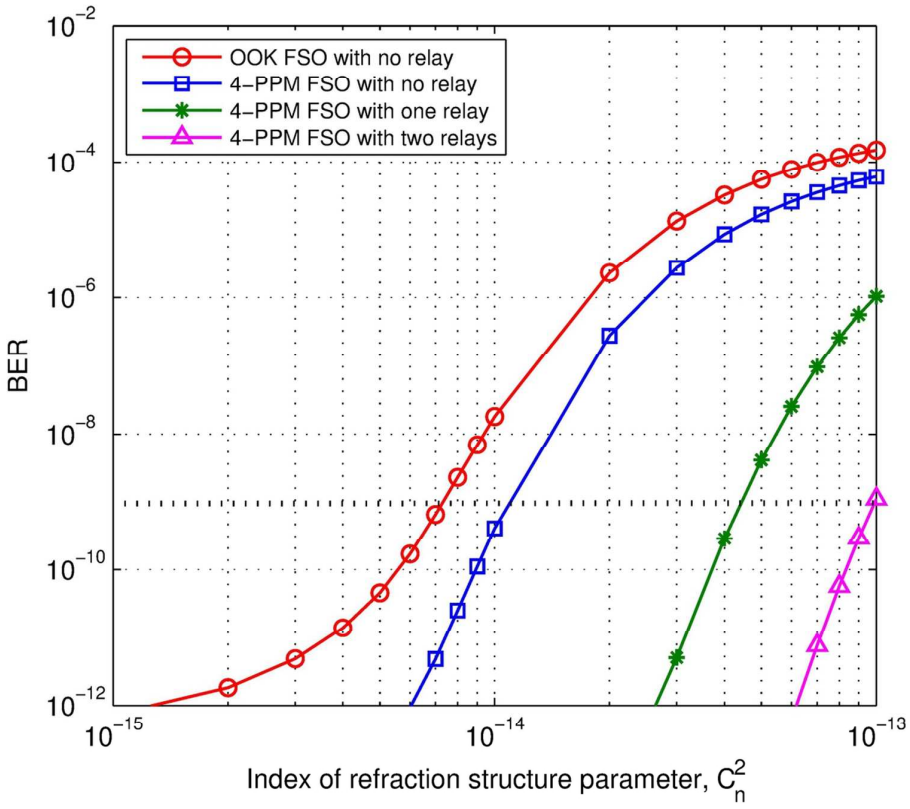

108x96mm (300 x 300 DPI)

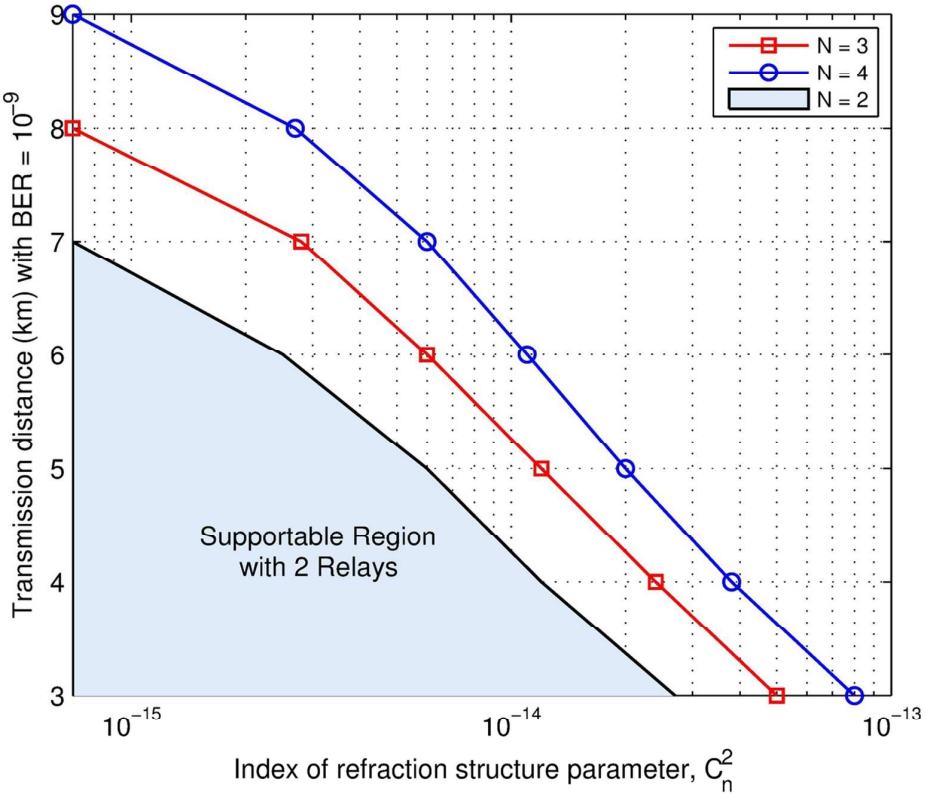

108x96mm (300 x 300 DPI)